The Journal of Engineering

The 14th IET International Conference on AC and DC Power Transmission (ACDC 2018)

IET Journals
The Institution of Engineering and Technology

Contingency-constrained optimisation method for operating urban power grids with flexible switching stations

eISSN 2051-3305
Received on 22nd August 2018
Accepted on 19th September 2018
E-First on 29th November 2018
doi: 10.1049/joe.2018.8449
www.ietdl.org

Jia Liu[1] ✉, Haozhong Cheng[1], Qian Xu[2], Zhou Lan[2], Pingliang Zeng[3], Liangzhong Yao[3]

[1]*Key Laboratory of Control of Power Transmission and Conversion, Ministry of Education, Shanghai Jiao Tong University, Shanghai, People's Republic of China*

[2]*State Grid Zhejiang Electric Power Corporation Economic Research Institute, Hangzhou, People's Republic of China*

[3]*China Electric Power Research Institute, Beijing, People's Republic of China*

✉ *E-mail: 714432724@qq.com*

Abstract: This study presents a multi-objective operation optimisation model for urban power grids with flexible switching (FS) stations to comprehensively improve system security and reliability. In the proposed model, uncertainties associated with load variation and component failures are considered. Moreover, constraints after a feeder or transformer $N-1$ contingency are preliminarily formulated. The operation problem optimises the apparent power of feeder section loading. The combination of normal boundary intersection and sequential quadratic programming is employed to solve the non-linear optimisation model. A case study carried out on a test 75-feeder distribution grid with FS stations demonstrates the effectiveness of the proposed model and solving method. Compared with conventional distribution loadability, the optimal load distribution solution obtained in this study provides a trade-off between system security and reliability. The coordinated operation optimisation method is suitable for urban smart distribution grids featured by distribution automation and large-scale interconnections.

1 Introduction

The operation optimisation problem for distribution systems aims at minimising objective functions by determining the optimal values for a set of decision variables [1]. With the integration of distributed generations, electric vehicles and energy storage devices, on the one hand, more component models should be incorporated when optimising system operation, on the other hand, the problem solving becomes more time consuming. Furthermore, the operation risk in distribution systems is sharply increased due to uncertainties associated with distributed generation output power and load variation [2]. Thus, a flexible distribution system operation optimisation model is urgently needed to guarantee system security and reliability under multiple uncertainties.

The sequential $N-1$ contingency testing is normally regarded as a system $N-1$ security assessment method [3]. However, this method can cost a lot of time to check system security after a component $N-1$ contingency, especially when the system is large. Moreover, in medium-voltage distribution systems, more interconnections of feeders are implemented and the loop structure has been primarily formed [4]. The available capacity of transformers in different substations can back up each other by the improved distribution feeder configuration. Under the condition of advanced distribution automation, the fault power can be restored among other adjacent substations. These changes further bound the application of conventional sequential $N-1$ contingency testing. Thus, in order to quantitatively provide system operators with the information of security margins, a region-wise methodology is proposed to assess system security [5, 6]. Chen *et al.* [5] present a distance-based security assessment method for power systems and provide a two-step solving algorithm to calculate the security distance. In [6], the region methodology is applied in distribution systems and an $N-1$ approximation method is proposed to observe the security region boundary. The topological characteristics of security region for distribution systems are summarised as follows: (i) the security region is a dense set; (ii) the security boundary is approximately linear and can be expressed by several hyperplanes.

Loadability is a fundamental index to evaluate both efficiency and reliability of a distribution system. In order to assess and optimise this index, a lot of studies have been reported in the literature [7–10]. In [7], a series of indices are defined to make the probabilistic evaluation of available loadability for radial distribution systems using Latin hypercube sampling-based Monte Carlo simulation and step-varied repeated power flow method. Aman *et al*. [8] present an optimal distribution system reconfiguration algorithm to maximise system loadability. In [9], a flexible evaluation method is proposed for urban distribution loadability considering transformer $N-1$ security. Xiao *et al.* [10] formulate an $N-1$ loadability model for interconnected distribution systems in the presence of a feeder or transformer $N-1$ contingency. The $N-1$ loadability operating point is just located on the security boundary [6].

All the above studies benefit a lot in the loadability evaluation and optimisation of distribution systems. However, the load distribution solutions in these existing works have not taken any indispensable security margins into account. Due to multiple uncertainties (e.g. distributed generation output power, load variation and component failures) in distribution systems, conventional distribution loadability cannot effectively guide the secure operation of distribution systems. Thus, it is of great importance to incorporate security margins into the loadability-based optimal operation model, which is a meaningful but ignored problem.

To alleviate the above problems, this paper proposes a multi-objective operation optimisation model for smart distribution grids in the presence of flexible switching (FS) stations to provide a trade-off between asset efficiency and system security. In the proposed model, the system security after a component (i.e. feeder or transformer) $N-1$ contingency is simultaneously guaranteed and optimised based on security distance. The system reliability is quantitatively evaluated using a defined $N-1$ loadability-based index. The optimal load distribution solution is obtained by a hybrid solving algorithm combining normal boundary intersection (NBI) and sequential quadratic programming (SQP). The main contribution of this paper is a novel operation optimisation model for interconnected distribution systems considering security distance and $N-1$ loadability, which has the following advantages: (i) a flexible, coordinated and precise model; (ii) system $N-1$ security and loadability optimisation; and (iii) good robustness in respect to the secure operation under uncertainties.

2 Model and algorithm for the optimal operation of distribution systems

2.1 Variation coefficient of security distance

The variation coefficient of security distance is a security distance-based margin index to quantitatively evaluate system $N-1$ security, which has been defined in [11]. Its mathematical expression is as follows:

$$V_{\mathrm{EVSD}} = \sum_{k=1}^{N_{\mathrm{FS}}} V_{\mathrm{SD}}^{k} / N_{\mathrm{FS}} \tag{1}$$

$$V_{\mathrm{SDSD}} = \sqrt{\sum_{k=1}^{N_{\mathrm{FS}}} \left(V_{\mathrm{SD}}^{k} - V_{\mathrm{EVSD}}\right)^{2} / N_{\mathrm{FS}}} \tag{2}$$

$$V_{\mathrm{VCSD}} = \frac{V_{\mathrm{SDSD}}}{V_{\mathrm{EVSD}}} \tag{3}$$

where V_{SD}^{k} is the security distance of feeder section F_k; V_{EVSD}, V_{SDSD}, and V_{VCSD} are, respectively, the expectation value, standard deviation, and variation coefficient of all security distances; and N_{FS} is the number of feeder sections in a specific distribution system.

V_{VCSD} can precisely evaluate the $N-1$ security and its margin of a distribution system under uncertainties [11]. Here, uncertainties related to demand and single component failure are considered in this paper. Smaller the V_{VCSD} is, higher is the $N-1$ security level of the whole distribution system.

2.2 N − 1 loadability adequacy

For an interconnected distribution system, the $N-1$ loadability adequacy is defined as the ratio of the real-time total load to $N-1$ loadability, which can be expressed as

$$V_{\mathrm{NLA}} = \frac{V_{\mathrm{RL}}}{V_{\mathrm{NL}}} \tag{4}$$

where V_{RL}, V_{NL}, and V_{NLA} are, respectively, the real-time total load, $N-1$ loadability, and $N-1$ loadability adequacy of a given distribution system. The method to obtain the $N-1$ loadability for a given interconnected distribution system has been specifically proposed in [10].

V_{NLA} represents the difference between the active total load and $N-1$ loadability, which is a quantitative evaluation index for system efficiency and reliability. When V_{NLA} is smaller than 1, it indicates that the efficiency and reliability of the system can be improved by integrating more loads. When V_{NLA} is bigger than 1, it represents that some components can be overloading after an $N-1$ contingency and some measures (e.g. network reconfiguration and load shedding) should be taken to decrease V_{NLA} in case of the system security constraint violation.

2.3 Problem formulation

The proposed distribution system operation optimisation model minimises the above-mentioned variation coefficient of security distance and $N-1$ loadability adequacy simultaneously, which are security and reliability dependent, respectively, and subjects to the normal operation constraints, feeder $N-1$ contingency constraints, and transformer $N-1$ contingency constraints. In the optimal operation problem, the decision variable is the apparent power of feeder section loading. The optimal load distribution solution obtained in this paper provides a trade-off between system security and reliability. The operation optimisation model for interconnected distribution systems can be formulated as

$$\begin{aligned} &\min\ (V_{\mathrm{VCSD}}, V_{\mathrm{NLA}}) \\ &\text{s.t.}\quad \text{normal operation constraints} \\ &\qquad \text{feeder } N-1 \text{ contingency constraints} \\ &\qquad \text{transformer } N-1 \text{ contingency constraints} \end{aligned} \tag{5}$$

It is worth mentioning that the coordinated operation optimisation scheme obtained from the above model is based on the assumption that the real-time load distribution among transformers and feeders is neglected. In fact, loads of transformers and feeders in a specific distribution system cannot always follow the ideal operating point. However, this optimal operating point offers an optimisation direction to the security and reliability of distribution systems, and some active management schemes (e.g. demand-side management and distribution feeder reconfiguration) can be flexibly taken to adjust the load distribution among transformers and feeders. The coordinated optimal operation mode can be approximately acquired when the load distribution matches with the ideal operating point, which achieves the operation optimisation for interconnected distribution systems with the consideration of both security and reliability. Moreover, the effects of switching of capacitors and transformer taps are considered in this paper when obtaining the optimal load distribution solution among feeders and transformers.

2.4 Constraints

2.4.1 Normal operation constraints:

$$S_F^k = \sum_{l=1} S_{f,\mathrm{tr}}^{k,l} \tag{6}$$

$$S_T^m = \sum_{F_k \in T_m} S_F^k \tag{7}$$

$$S_{f,zfc}^k = \frac{\left(\left|S_F^k \cos\varphi\right|\right)^2 + \left(\left|S_F^k \sin\varphi\right|\right)^2}{\left(U_{zc}^k\right)^2} (Rl_k + \mathrm{j}Xl_k) \tag{8}$$

$$\begin{aligned} \Delta U_{zc}^{k(j+1)} = [&(\left|S_F^k\right| \cos\varphi + \mathrm{Re}(S_{f,zfc}^k))Rl_k \\ &+(\left|S_F^k\right| \sin\varphi + \mathrm{Im}(S_{f,zfc}^k))Xl_k]/U \end{aligned} \tag{9}$$

$$\begin{aligned} \delta U_{zc}^{k(j+1)} = [&(\left|S_F^k\right| \cos\varphi + \mathrm{Re}(S_{f,zfc}^k))Xl_k \\ &-(\left|S_F^k\right| \sin\varphi + \mathrm{Im}(S_{f,zfc}^k))Rl_k]/U \end{aligned} \tag{10}$$

$$U_{zc}^{k(j+1)} = \sqrt{\left(U - \Delta U_{zc}^{k(j+1)}\right)^2 + \left(\delta U_{zc}^{k(j+1)}\right)^2} \tag{11}$$

$$U_{\min} \le U_{zc}^{k(j+1)} \le U_{\max} \tag{12}$$

where S_F^k is the load of F_k; $S_{f,\mathrm{tr}}^{k,l}$ is the load transferred from F_k to F_l when F_k faults; $S_{f,zfc}^k$ is the network loss of F_k under normal operation; φ is the power factor angle under normal operation; R and X are, respectively, the unit resistance and reactor of conductors; l_k is the line length of F_k; U_{zc}^k is the voltage of F_k under normal operation; U_{zc}^k is the voltage of F_k under normal operation; ΔU_{zc}^k and δU_{zc}^k are, respectively, the longitudinal and transverse components of voltage drop of F_k under normal operation; $U_{\min}$ and $U_{\max}$ are, respectively, the lower and upper limits of bus voltage; and j is the number of iterations.

Equations (6) and (7) are, respectively, the loading calculation constraints of feeders and transformers. Equation (8) is the feeder loss calculation constraint in a normal state. Equations (9) and (10) are the calculation constraints of longitudinal and transverse components of voltage drop in a normal state, respectively. Equations (11) and (12) are, respectively, the calculation and limit constraints of voltage magnitude in a normal state.

2.4.2 Feeder N − 1 contingency constraints:

$$S_{f,\text{loss}}^{k,l}=\frac{\left(\left|S_{f,\text{tr}}^{k,l}\cos\varphi'\right|\right)^2+\left(\left|S_{f,\text{tr}}^{k,l}\sin\varphi'\right|\right)^2}{\left(U_k^{k,l}\right)^2}(Rl_{kl}+\text{j}Xl_{kl}) \tag{13}$$

$$\begin{aligned}S_{f,fc}^{k,l}=[(&\left|S_{f,\text{tr}}^{k,l}+S_F^lL_{kl}\right|\cos\varphi'+\text{Re}(S_{f,\text{loss}}^{k,l}))^2+(\left|S_{f,tr}^{k,l}\right.\\&\left.+S_F^lL_{kl}\right|\sin\varphi'+\text{Im}(S_{f,\text{loss}}^{k,l}))^2]\cdot(Rl_l+\text{j}Xl_l)/(U_l^{k,l})^2\end{aligned} \tag{14}$$

$$\left|S_{f,\text{tr}}^{k,l}+S_F^l+S_{f,fc}^{k,l}+S_{f,\text{loss}}^{k,l}\right|\le S_{F,\max}^l \tag{15}$$

$$\begin{aligned}\Delta U_l^{k,l(j+1)}=[(&\left|S_{f,\text{tr}}^{k,l}+S_F^lL_{kl}\right|\cos\varphi'+\text{Re}(S_{f,\text{loss}}^{k,l}\\&+S_{f,fc}^{k,l}))Rl_l+(\left|S_{f,\text{tr}}^{k,l}+S_F^lL_{kl}\right|\sin\varphi'\\&+\text{Im}(S_{f,\text{loss}}^{k,l}+S_{f,fc}^{k,l}))Xl_l]/U\end{aligned} \tag{16}$$

$$\begin{aligned}\delta U_l^{k,l(j+1)}=[(&\left|S_{f,tr}^{k,l}+S_F^lL_{kl}\right|\cos\varphi'+\text{Re}(S_{f,\text{loss}}^{k,l}\\&+S_{f,fc}^{k,l}))Xl_l-(\left|S_{f,tr}^{k,l}+S_F^lL_{kl}\right|\sin\varphi'\\&+\text{Im}(S_{f,\text{loss}}^{k,l}+S_{f,fc}^{k,l}))Rl_l]/U\end{aligned} \tag{17}$$

$$U_l^{k,l(j+1)}=\sqrt{\left(U-\Delta U_l^{k,l(j+1)}\right)^2+\left(\delta U_l^{k,l(j+1)}\right)^2} \tag{18}$$

$$\begin{aligned}\Delta U_k^{k,l(j+1)}=[(&\left|S_{f,\text{tr}}^{k,l}\right|\cos\varphi'+\text{Re}(S_{f,\text{loss}}^{k,l}))Rl_{kl}\\&+(\left|S_{f,\text{tr}}^{k,l}\right|\sin\varphi'+\text{Im}(S_{f,\text{loss}}^{k,l}))Xl_{kl}]/U_l^{k,l(j+1)}\end{aligned} \tag{19}$$

$$\begin{aligned}\delta U_k^{k,l(j+1)}=[(&\left|S_{f,\text{tr}}^{k,l}\right|\cos\varphi'+\text{Re}(S_{f,\text{loss}}^{k,l}))Xl_{kl}\\&-(\left|S_{f,\text{tr}}^{k,l}\right|\sin\varphi'+\text{Im}(S_{f,\text{loss}}^{k,l}))Rl_{kl}]/U_l^{k,l(j+1)}\end{aligned} \tag{20}$$

$$U_k^{k,l(j+1)}=\sqrt{\left(U_l^{k,l(j+1)}-\Delta U_k^{k,l(j+1)}\right)^2+\left(\delta U_k^{k,l(j+1)}\right)^2} \tag{21}$$

$$U_{\min}\le U_k^{k,l(j+1)}\le U_{\max} \tag{22}$$

where $S_{f,\text{loss}}^{k,l}$ is the network loss of the FS station between F_k and F_l after loads distributed on F_l when F_k faults; $S_{f,fc}^{k,l}$ is the network loss of F_l after loads distributed on F_l when F_k faults; $S_{F,\max}^l$ is the capacity of F_l; φ' is the power factor angle after restoration; l_{kl} is the line length of the tie line between F_k and F_l; L_{kl} is the tie relationship between F_k and F_l, which takes the value 1 if this connection exists and 0 otherwise; $U_k^{k,l}$ is the voltage of F_k after loads distributed on F_l when F_k faults; $\Delta U_k^{k,l}$ and $\delta U_k^{k,l}$ are, respectively, the longitudinal and transverse components of voltage drop of F_k after loads distributed on F_l when F_k faults.

Equations (13) and (14) are, respectively, the loss calculation constraints of the branch between F_k and F_l, and F_l in $N-1$ state. Equation (15) is the feeder capacity constraint in $N-1$ state. Equations (16) and (17) are the calculation constraints of longitudinal and transverse components of the voltage drop of F_l in $N-1$ state, respectively. Equation (18) is the voltage magnitude calculation constraint of F_l in $N-1$ state. Equations (19) and (20) are the calculation constraints of longitudinal and transverse components of the voltage drop of F_k in $N-1$ state, respectively. Equation (21) is the voltage magnitude calculation constraint of F_k in $N-1$ state. Equation (22) is the voltage magnitude constraint in $N-1$ state.

2.4.3 Transformer N − 1 contingency constraints:

$$S_{T,\text{tr}}^{m,n}=\sum_{F_k\in T_m,F_l\in T_n}(S_{f,\text{tr}}^{k,l}+S_{f,\text{loss}}^{k,l}+S_{f,fc}^{k,l}) \tag{23}$$

$$\left|S_{T,\text{tr}}^{m,n}+S_T^n+\sum_{F_l\in T_n}S_{f,zfc}^l+\sum_{F_k\in T_m,F_l\in T_n}(S_{f,zfc}^lL_{kl})\right|\le S_{T,\max}^n \tag{24}$$

where $S_{T,\text{tr}}^{m,n}$ is the load transferred from the transformer T_m to T_n when T_m faults; S_T^n is the load of T_n; and $S_{T,\max}^n$ is the capacity of T_n.

Equation (23) is the load transfer calculation constraint in $N-1$ state. Equation (24) is the transformer capacity constraint in $N-1$ state.

2.5 Solution algorithm

The optimal operation model proposed above is a multi-objective non-linear optimisation problem including multiple variables. Thus, it is pretty difficult to obtain the optimal load distribution solution using a single algorithm. A hybrid algorithm combining NBI and SQP is employed to solve the problem.

The theory of Pareto optimality has been widely applied to solve multi-objective optimisation problems. The NBI method is an effective method to form the solution set of uniform Pareto front end in the criterion space. The Pareto solutions formed are generally evenly distributed and produce a more accurate representation of the trade-off surface [12]. The procedure of NBI method is as follows:

Step 1: The payoff matrix $\boldsymbol{P}$ is formed to map the weighting vectors to the objective space ψ, which can be expressed as

$$\boldsymbol{P}=[\psi_1,\psi_2]=\begin{bmatrix}F(x_1) & F(x_2)\\ f(x_1) & f(x_2)\end{bmatrix} \tag{25}$$

where the diagonal elements referred as ideal values represent the optimal objective values considering $F(x)$ and $f(x)$, respectively.

Step 2: Divide the utopia line between ψ_1 and ψ_2 into n equal slices and then project at the point of the kth section in the direction of the normal vector to form the Pareto surface.

Step 3: Maximise the distance between the utopia line and the Pareto surface according to the Pareto optimality condition.

The original optimisation problem in (5) is transformed into a set of the parameterised single-objective optimisation problems with the objective to maximise the distance between the utopia line and the trade-off surface.

The SQP method has been widely applied to solve the non-linearly constrained optimisation problems, which has the advantages of the super-linear convergence rate, global convergence and high computation efficiency [13]. The fundamental idea of the SQP approach is to substitute the original model for a quadratic programming sub-problem at the current iteration and then use the minimiser of this sub-problem to define a new iteration [14]. The detailed procedure of SQP has been described in [14], which is regarded as an application of the Newton's method to the Karush-Kuhn-Tucher optimality conditions for the original problem.

The flowchart of the hybrid algorithm to solve the coordinated optimal model is shown in Fig. 1.

3 Case study

In order to obtain the optimal operation mode and validate the effectiveness of the formulated problem and solution algorithm, the test 75-feeder distribution system with FS stations [15] is applied to the case study and analysis. The parallelised programs are compiled in MATLAB R2014a and run on a PC with 3.00 GHz CPU and 4 GB RAM.

Fig. 2 shows the test distribution system containing 4 substations, 8 transformers, 75 feeders and 24 FS stations. The rated voltage at the root of a feeder is 10.5 kV. The average system load factor is 0.364. The load types are all the same with power factor 0.85. The version of feeders is LGJ-185. The rated capacity, length, unit resistance, and unit reactor of each feeder are, respectively, 8.92 MVA, 4.65 km, 0.163, and 0.365 Ω. The switchable capacitor banks are installed at the end of feeders and the total reactive power capacity of switchable capacitor banks in the test system is 48.4 MVAr.

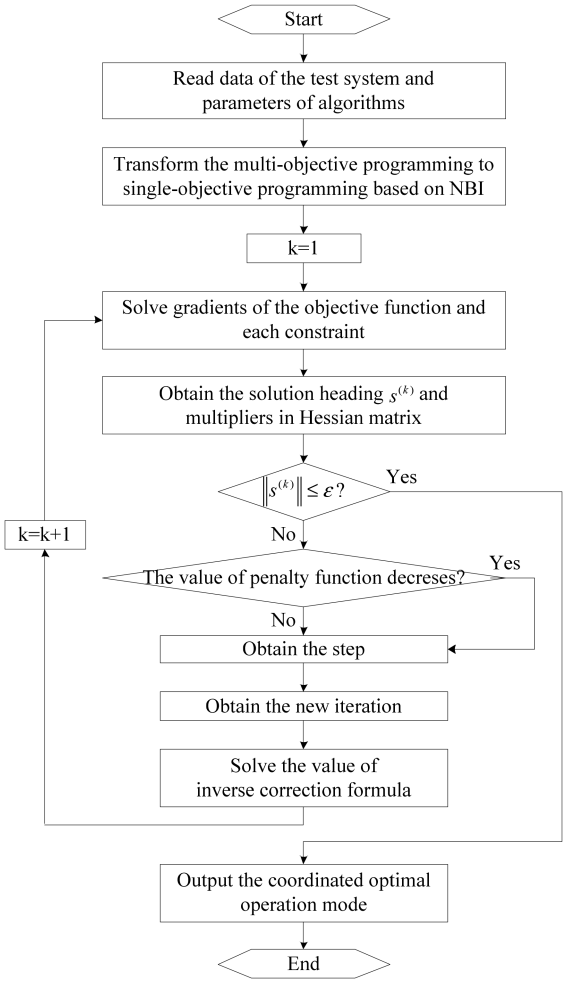

Fig. 1 *Flowchart for solving the coordinated optimal model*

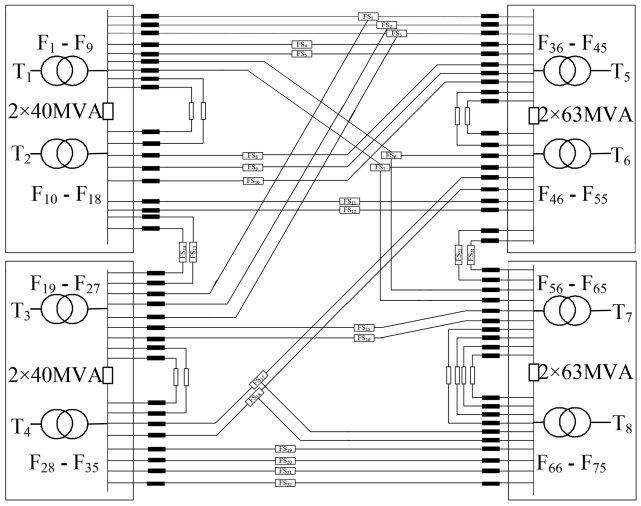

Fig. 2 *Test distribution system*

Two cases are analysed for comparison purpose. The cases are described as follows:

Case 1: Considering the variation coefficient of security distance in the operation optimisation model.
Case 2: Without considering the variation coefficient of security distance in the operation optimisation model.

3.1 Results of the proposed operation optimisation (Case 1)

The load distribution among transformers and feeders and security distance for this case are, respectively, shown in Tables 1 and 2. At this operating point, the average load factor of the test system is 0.612.

It can be observed from Table 1 that the result of $N-1$ loadability for this case in the presence of security margins is 252.2 MVA while the result for the real operation state is 150 MVA, which validates that the efficiency and reliability of the system have been greatly improved through the optimisation compared with the real operation state. As seen from Table 2, all security distances for this case are positive, which indicates that the operating point obtained in this paper not only can guarantee system $N-1$ security, but also has a certain quantity of margins to security region boundaries.

3.2 Comparisons of the two cases

Compared with the operation mode for Case 1, the operation mode for Case 2 is also solved using the execution of the proposed procedure in Section 2.5. The result of $N-1$ loadability for this case under this circumstance is 302.0 MVA and the average load factor of the test system at this point is 0.733, which is larger than the result with the consideration of security margin.

Comparisons of evaluation indices for Cases 1 and 2 are illustrated in Table 3. From Table 3, it can be observed that the formulated operation mode can provide a trade-off between asset efficiency and system security. The following reason is analysed: from the perspective of system security, the V_{EVSD} and V_{SDSD} of the operation mode for Case 1 are, respectively, 1.6 and 1.3 MVA, which illustrate the $N-1$ security of the operating point and the sufficiency of security margin to integrate appropriate loads on each feeder. As a contrast, the security distances V_{EVSD} and V_{SDSD} of the operation mode for Case 2 are all zero. The results indicate that the operating point under this mode is just located on the security region boundary, which has difficulty in guaranteeing the $N-1$ secure operation of the test system under uncertainties associated with distributed generation output power and load variation; from the perspective of asset efficiency, although the V_{NLA} of the operation mode for Case 1 is 0.09 bigger than that without the consideration of security margin, this deviation could be within the acceptable range of asset efficiency in practical application. Thus, the proposed operation mode in this paper could be better considering both system security and asset efficiency.

3.3 N − 1 security margin verification with load variation

Assuming load variation on each feeder with 0.01 MVA increases for the operating point without considering security margin, all security distances for this case are negative, which indicate that the operating point after little load growth is outside security region and cannot guarantee system $N-1$ security. For example, the security distance of F_1 is −0.02 MVA. As a contrast, after the load of each feeder increases by 0.01 MVA from the operating point considering security margin, the security distances for this case are calculated and shown in Fig. 3.

As seen in Fig. 3, all security distances for this case under this circumstance are positive. This result indicates that the corresponding operating point after load growth is inside the security region and can guarantee system $N-1$ security. This is because the security distance of each feeder for the operation mode considering security margin is larger than the sum growth of load and power loss on the corresponding feeder. Thus, the operation mode formulated in this paper has sufficient security margins to guarantee the secure operation of the test distribution system under uncertainties on the premise of high asset efficiency and can be utilised for a practical operation application.

4 Conclusion

In this paper, a coordinated operation optimisation model for interconnected distribution systems is proposed to improve system security and reliability after a feeder or transformer $N-1$ contingency. The proposed model optimises the apparent power of feeder section loading. Two objectives (i.e. a variation coefficient of security distance and $N-1$ loadability adequacy) are minimised

Table 1 Load distribution among transformers and feeders

No.	Transformer loading, MVA	Feeder loading, MVA									
		1	2	3	4	5	6	7	8	9	10
1	25.8	2.3	2.3	2.3	3.2	3.2	2.0	2.0	4.3	4.3	—
2	27.5	3.9	3.9	1.7	1.7	1.7	3.1	3.1	4.2	4.2	—
3	27.7	3.9	4.0	1.7	1.7	1.7	3.4	3.4	3.8	3.8	—
4	24.2	4.4	4.4	1.2	1.2	3.3	3.3	3.3	3.3	—	—
5	36.5	5.2	5.2	5.2	2.1	2.1	3.2	3.2	3.2	3.6	3.6
6	49.2	3.6	3.6	5.3	5.3	6.8	6.8	4.8	4.8	4.1	4.1
7	45.1	3.4	3.4	5.3	5.3	3.9	3.9	5.0	5.0	5.0	5.0
8	25.3	2.2	2.2	2.2	2.2	4.3	4.3	1.9	1.9	1.9	1.9

Table 2 Security distance of each feeder

No.	Security distance, MVA									
	1	2	3	4	5	6	7	8	9	10
1	0.8	0.8	0.8	3.3	3.3	1.0	1.0	0.1	0.1	—
2	0.1	0.1	3.8	3.8	3.8	0.4	0.4	0.1	0.2	—
3	0.2	0.1	1.5	1.5	1.5	1.1	1.1	0.1	0.1	—
4	0.1	0.1	3.0	3.0	3.5	3.5	3.5	3.5	—	—
5	1.5	1.5	1.5	3.3	3.3	3.8	3.8	3.8	1.2	1.2
6	1.2	1.2	1.0	1.0	0.1	0.1	0.4	0.4	0.9	0.9
7	0.9	0.9	1.0	1.0	1.1	1.1	1.2	1.2	1.2	1.2
8	1.2	1.2	1.2	1.2	3.0	3.0	3.5	3.5	3.5	3.5

Table 3 Comparisons of results for Cases 1 and 2

Method	V_{NLA}	Transformer loading, MVA								V_{EVSD}, MVA	V_{SDSD}, MVA	V_{VCSD}
		1	2	3	4	5	6	7	8			
Case 1	0.59	25.8	27.5	27.7	24.2	36.5	49.2	45.1	25.3	1.6	1.3	0.81
Case 2	0.50	30.4	31.3	32.2	26.3	47.5	60.4	59.6	25.2	0	0	—

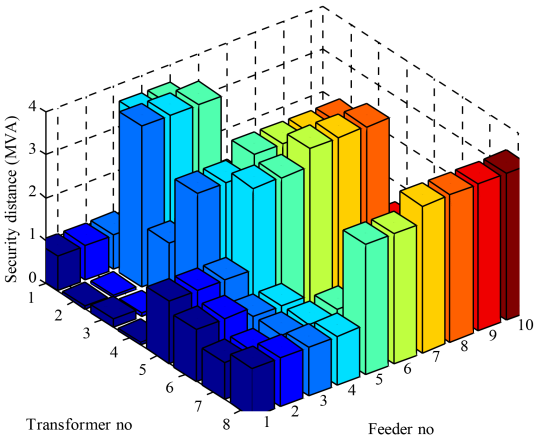

Fig. 3 *Security distance for the test system after load growth*

using the combination of NBI and SQP algorithms. The case study carried out on a test 75-feeder distribution system validates the feasibility of the defined indices, proposed model, and solving method. The simulation results demonstrate that it is possible to determine the optimal operation mode using the flexible, coordinated, and precise model. The optimal operation model proposed in this paper could not only provide a trade-off between system security and reliability, but also own good robustness in respect to the practical operation under uncertainties.

5 Acknowledgments

This work was supported by the National Key Research and Development Program of China (2016YFB0900102) and Science and Technology Program of State Grid Corporation of China (5211JY160004).

6 References

[1] Macedo, L.H., Franco, J.F., Rider, M.J., *et al.*: 'Optimal operation of distribution networks considering energy storage devices', *IEEE Trans. Smart Grid*, 2015, **6**, (6), pp. 2825–2836

[2] Xing, H., Cheng, H., Zhang, Y., *et al.*: 'Active distribution network expansion planning integrating dispersed energy storage systems', *IET Gener. Transm. Distrib.*, 2016, **10**, (3), pp. 638–644

[3] Sidhu, T.S., Cui, L.: 'Contingency screening for steady-state security analysis by using FFT and artificial neural networks', *IEEE Trans. Power Syst.*, 2000, **15**, (1), pp. 421–426

[4] Zhao, Y., An, Y., Ai, Q.: 'Research on size and location of distributed generation with vulnerable node identification in the active distribution network', *IET Gener. Transm. Distrib.*, 2014, **8**, (11), pp. 1801–1809

[5] Chen, S., Chen, Q., Xia, Q., *et al.*: 'Steady-state security assessment method based on distance to security region boundaries', *IET Gener. Transm. Distrib.*, 2013, **7**, (3), pp. 288–297

[6] Xiao, J., Zu, G., Gong, X., *et al.*: 'Observation of security region boundary for smart distribution grid', *IEEE Trans. Smart Grid*, 2017, **8**, (4), pp. 1731–1738

[7] Zhang, S., Cheng, H., Zhang, L., *et al.*: 'Probabilistic evaluation of available load supply capability for distribution system', *IEEE Trans. Power Syst.*, 2013, **28**, (3), pp. 3215–3225

[8] Aman, M.M., Jasmon, G.B., Bakar, A.H.A., *et al.*: 'Optimum network reconfiguration based on maximization of system loadability using continuation power flow theorem', *Int. J. Electr. Power Energy Syst.*, 2014, **54**, pp. 123–133

[9] Luo, F., Wang, C., Xiao, J., *et al.*: 'Rapid evaluation method for power supply capability of urban distribution system based on $N-1$ contingency analysis of main-transformers', *Int. J. Electr. Power Energy Syst.*, 2010, **32**, (10), pp. 1063–1068

[10] Xiao, J., Liu, S., Li, Z., *et al.*: 'Loadability formulation and calculation for interconnected distribution systems considering $N-1$ security', *Int. J. Electr. Power Energy Syst.*, 2016, **77**, pp. 70–76

[11] Liu, J., Cheng, H., Tian, Y., *et al.*: 'Stochastic multi-objective distribution feeder reconfiguration based on point estimation considering $N-1$ security and net loss'. Proc. IEEE Power and Energy Society General Meeting, Boston, USA, July 2016, pp. 1–5

[12] Das, I., Dennis, J.E.: 'Normal-boundary intersection: A new method for generating the Pareto surface in nonlinear multicriteria optimization problems', *SIAM J. Optim.*, 1998, **8**, (3), pp. 631–657

[13] Subathra, M.S.P., Selvan, S.E., Victoire, T.A.A., *et al.*: 'A hybrid with cross-entropy method and sequential quadratic programming to solve economic load dispatch problem', *IEEE Trans. Power Syst.*, 2015, **9**, (3), pp. 1031–1044

[14] Nocedal, J., Wright, S.J.: '*Sequential quadratic programming*' (Springer Press, New York, 2006)

[15] Xiao, J., Gang, F., Huang, R., *et al.*: 'Total supply capability model for flexible distribution network', *Autom. Electr. Power Syst.*, 2017, **41**, (5), pp. 30–38